Coating on a Rough Surface

Andrew Clarke
Kodak Limited, Harrow, Middelsex, HA1 4TY, U.K.

Commercial products such as photographic materials and speciality papers manufactured by single or multilayer coating processes, all have some surface topographic structure. Nevertheless, for many materials, a uniform plane approximates their surface, and analyses of dynamic wetting, a fundamental physical process which determines coating process limits, usually assume this condition. It is demonstrated here that under certain combinations of coating process parameters, the maximum coating speed is not predicted even qualitatively by using this assumption. Furthermore, the experiments indicate that a second coating mechanism supersedes complete wetting and promotes extremely high coating speeds.

Introduction

Liquid coating methods are employed to manufacture products as diverse as chocolates and television screens. Coating is the practical application of the fundamental physical process of spreading a liquid on a surface. This fundamental process underpins many other applications in addition to coating, such as printing, painting and spraying of insecticides, and so on. Thus, the fundamental understanding of dynamic wetting (Blake, 1993; Blake and Ruschak, 1997) leads to the understanding of a wide range of technologically important applications.

For many liquids and solids, the liquid will partially wet the substrate giving a well-defined drop. A distinct three-phase line, where the substrate and the two fluids meet, defines the drop perimeter. In equilibrium, Young's equation may be applied which relates the three interfacial tensions, solid/liquid, solid/air and liquid/air, to the static contact angle. When a liquid is forced to spread on a substrate in air, the contact angle will change; for angles measured through the liquid, the angle will increase as the liquid is forced to displace the air. When this dynamic advancing contact angle approaches 180°, air begins to be entrained between the liquid and the substrate. In a manufacturing environment this phenomena usually leads to a failure of the coating process. Despite this technological importance, there is still a large degree of uncertainty that surrounds the dynamics of wetting, even on a smooth uniform surface. With a single exception (Shikhmurzaev, 1997), the literature contains two classes of model: those that ignore the processes occurring at the three-phase line and use the formalism of continuum hydrodynamics (Voinov, 1976; Cox, 1986), and models that employ statistical mechanics to describe the dynamic contact angle, but ignore the hydrodynamics (Blake et al., 1993; Blake and Ruschak, 1997). A common feature of these models and associated experiments is that the air-entrainment speed is found to be inversely related to the viscosity of the liquid at the wetting line (Blake and Ruschak, 1997; Gutoff and Kendrick, 1982; Burley and Jolly, 1984). Thus, for a high-speed coating process, the ultimate coating speed is understood to be closely related to the viscosity of the liquid adjacent to the substrate as it is entrained (Blake et al., 1993).

Many studies of static wetting on rough surfaces have been made (for example, Rolley et al., 1998; Johnson and Dettre, 1964; Dettre and Johnson, 1964; Herminghaus, 2000; Palasantzas, 1995; Zhou and Th. M., 1995). In addition, there have been several investigations of sliding drops on rough surfaces: (Menchaca-Rocha, 1992) for mercury drops and, more recently, Miwa et al. (2000) for water drops on hydrophobic surfaces. In these dynamic systems, it was found that as the roughness was increased, there was less contact between the drop and the substrate, so frictional forces were lower and the drop moved more easily. However, outside of the patent literature (Clarke et al., 1998; Suga et al., 1993) and one plunging tape experiment (Buonopane et al., 1986), no systematic studies of high-speed coating on rough surfaces have been published.

The coating of a rough support is expected to proceed in one of two ways (Blake and Ruschak, 1997):

(1) The liquid completely wets the surface, that is, the wetting line moves up and down the peaks and valleys which characterize the roughness. Since the wetting line has to travel

further than it would over a smooth surface for an equivalent macroscopic length of substrate, the maximum achievable coating speed will be lower. Consider, for example, a sinusoidal topography with unit amplitude and wavelength 2π: here, the distance along the curve will be approximately 1.2 times the distance along a line defining the mean height. Therefore, there will be an expected decrease in speed for the onset of wetting failure, with the speed on the rough support being approximately 82% of the speed on a chemically equivalent, but perfectly smooth, support.

(2) Instead of completely wetting the surface, the liquid only attaches at the peaks (Johnson and Dettre, 1964; Dettre and Johnson, 1964; Herminghaus, 2000; Menchaca-Rocha, 1992; Miwa et al., 2000). This is expected if, for example, the liquid bridges to the next peak before it can wet the intervening valley. Skipping from peak to peak will occur when the substrate speed is comparable with or greater than the maximum wetting speed on the corresponding smooth support. In addition, the implicit air film (disrupted into air pockets) must be smaller than the scale of the roughness or else macroscopic coating failure will ensue.

In what follows it is shown that, depending on the coating parameters chosen, each of these mechanisms is able to operate.

Experimental Studies

All the experiments described here were performed on an apparatus consisting of a substrate drive and a coating device. This apparatus, shown in Figure 1, has been described previously (Blake et al., 1994). In brief, the drive is configured to convey a 35 mm wide tape at speeds from less than 0.01 m/s to greater than 10 m/s with an accuracy of $\pm 1\%$. The coating device is a symmetrical 4 slot die (Blake and Ruschak, 1997, p. 465), which has the experimental advantage of providing a sheet of liquid, a curtain, that falls vertically independent of flow rate (Clarke et al., 1997).

The substrates used in this study were smooth poly(ethyleneterephthalate) (PET) and variously rough polyethylene coated papers (PE). The roughness of each surface was assessed using a WYKO 2000 scanning optical microscope. In particular the surfaces are characterized by a 10 point average peak-to-peak height R_Z (DIN 4768; ISO 4287). The liquids used were various concentrations of aqueous gelatin (Eastman Chemicals) and various concentrations of aqueous glycerol (Fisons, SLR or Croda, BP). In both cases, 0.3 % w/w of an inert blue dye was added to aid observation of air-entrainment.

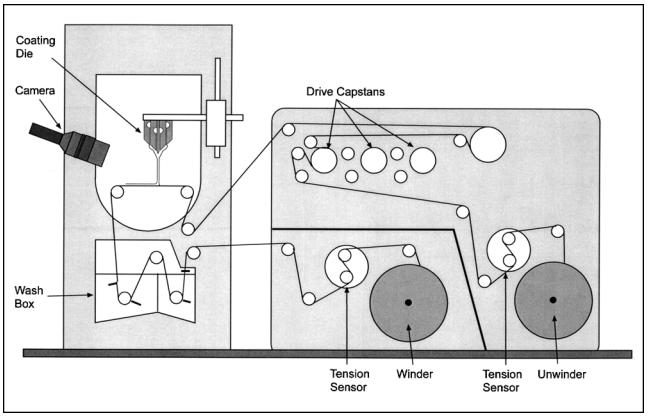

Figure 1. Experimental arrangement.

Note the camera location with respect to Figures 4 and 5.

Coatings were made as single layers and were observed just downstream of the wetting line using a standard CCD video camera (Pulnix TM-765E) and synchronized strobe lamp (EG &G MVS-7060). Each experiment was recorded using a VCR (Panasonic AG-7330 S-VHS) for subsequent analysis. Machine parameters such as speed and flow rate were simultaneously logged using a PC equipped with a multifunction I/O card (National Instruments NB-MIO-16E). The two records (video and PC datalog) were linked using a timecode generator, which was simultaneously read by the computer and used to embed a field index in the video recording. Illumination provided via a Fostec fiber optic bundle from the strobe lamp gave an 8 μs light pulse, short enough to eliminate motion blur and allow observation of individual bubbles. The two substrates required different lighting arrangements: PET is transparent and was observed in dark-field mode so that wetting failure could be discerned easily as bright bubbles on a black background. PE coated paper is white, and, therefore, wetting failure was observed via density differences and disturbances in the light reflected from the substrate.

Results

In a typical curtain coating process with liquid viscosity η, substrate speed S, surface tension γ, liquid density ρ, flow rate per unit width Q, curtain height h, and curtain velocity $U\ [=\sqrt{(2gh)}]$, the Capillary number ($Ca = \eta S/\gamma$) is O(1), the Weber number ($We = \rho QU/\gamma$) is O(10) and, therefore, the modified Reynolds number ($Re = We/Ca = \rho QU/\eta S$) is O(10). Here the speed of onset of wetting failure was measured as a function of liquid viscosity, curtain flow rate, and curtain height for various substrate roughnesses. We choose to plot our data as flow rate per unit width of coating vs. substrate speed. Such a plot or coating "map" displays several generic regions of behavior already described elsewhere (Blake and Ruschak, 1997). To summarize, at low flow rates, the curtain is unstable and will not form; at high flow rates, a recirculating region of liquid forms behind the curtain (Clarke, 1995). As speed is increased, a breakdown of the coating process eventually occurs which is often referred to as air-entrainment or wetting failure. The substrate speed at the onset of air entrainment is usually highest at intermediate flow rates. Under certain conditions, coating may be metastable with respect to air entrainment, such that the onset of air entrainment as speed is increased occurs at a significantly higher coating speed than that at which it clears. This we refer to as coating hysteresis.

Figure 2 shows four graphs: low and high viscosity aqueous gelatin solutions coated on a smooth substrate (PET), and low and high viscosity aqueous gelatin solutions coated on a rough substrate ($R_Z = 4.4\ \mu$m). The smooth substrate at low viscosity (a), shows a coating map with some hysteresis at high flow rates. Comparing (a) with the map for a high viscosity liquid on the same substrate (b), we see that there is a reduc-

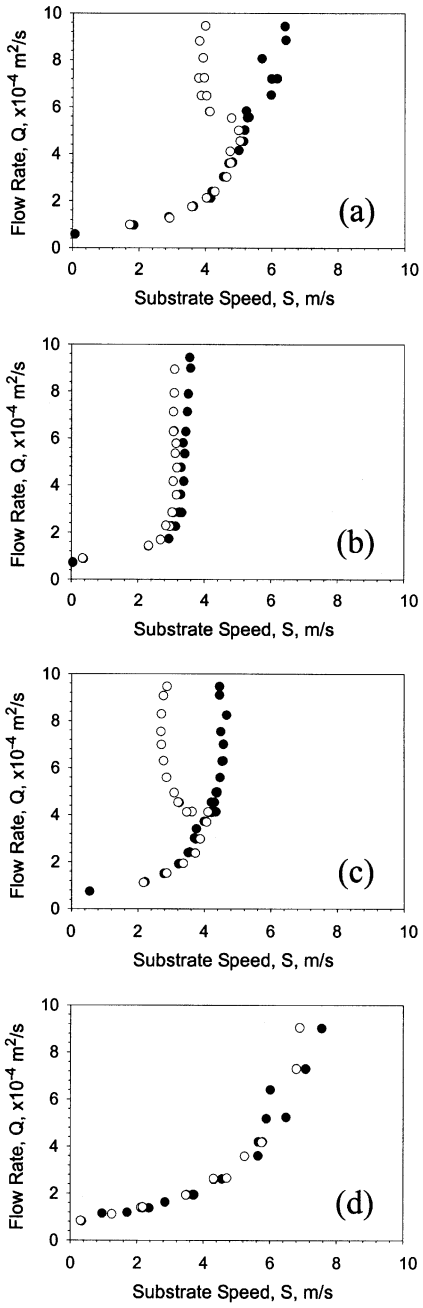

Figure 2. Interaction between roughness and liquid viscosity.

The liquid is aqueous gelatin +3% blue dye, the curtain height is 70 mm, the application angle is +45°. Onset of wetting failure on increasing web speed (●); disappearance of wetting failure on reducing web speed (○. (a) Low shear viscosity $\eta = 21.8$ m Pas, roughness $R_Z = 0.6$ μm; (b) $\eta = 171$ mPas, $R_Z = 0.6$ μm; (c) $\eta = 21.8$ mPas, $R_Z = 4.4$ μm; (d) $\eta = 171$ mPas, $R_Z = 4.4$ μm.

tion in the speed for the onset of air entrainment. This reduction is in accord with our understanding of dynamic wetting at the higher viscosity: that is, that the air-entrainment speed is inversely related to the viscosity of the liquid at the wetting line (Blake and Ruschak, 1997) and that, therefore, higher viscosity implies lower speed. Comparing map (a) with

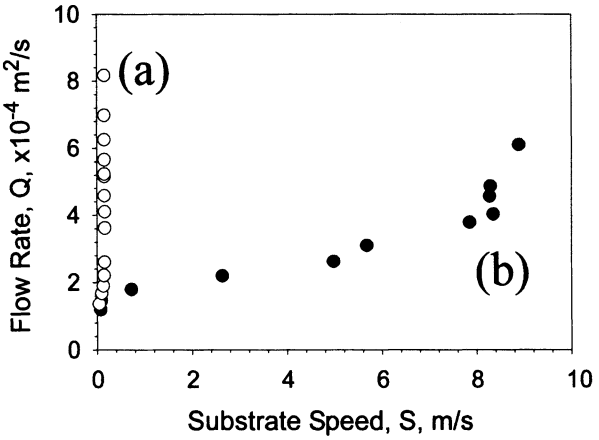

Figure 3. Coating of a Newtonian liquid (208 m·Pa·s aqueous glycerol).

(a) Onto smooth ($R_Z = 0.6$ μm) PET surface (○); (b) onto rough ($R_Z = 6.8$ μm) PE surface (●). The coating conditions (30 mm curtain height, 0° application angle) were identical for both cases.

the map obtained for the same viscosity but a rough support (c), there is a decrease in the speed for the onset of air entrainment. Again, this reduction is as expected since in covering this surface, the liquid has to wet a greater area, and, thus, the same maximum speed of wetting implies a lower effective coating speed. Finally, (d) shows the coating map obtained for a high viscosity liquid coated on a rough support. Comparing (d) with (c), there is a very significant speed increase on increasing the viscosity. This is in direct contradiction both to the effect previously observed on a smooth substrate ((b) and (a)), and conventional models of dynamic wetting. Comparing (d) and (b), there is again a substantial speed increase; since, between (d) and (b), the primary change is the substrate topography, we postulate that the liquid is wetting less area and is simply wetting each asperity in turn. This is a dynamic analogue of arguments put forward by Johnson and Dettre (1964) and more recently Herminghaus (2000).

The effect observed on a rough support in Figure 2 is demonstrated more dramatically with a Newtonian liquid. Figure 3 shows two coating maps: (a) on a smooth surface (PET) and (b) on a rough surface ($R_Z = 6.8$ μm). The coating liquid (208 mPas aqueous glycerol) and coating conditions were identical for cases (a) and (b), yet there are nearly two orders of magnitude difference in the onset speeds of wetting failure. For a Newtonian liquid of this viscosity, the lower speed observed on the smooth substrate (a) would be that expected from dynamic wetting observations (Blake, 1993).

Figure 4 shows the morphology of the observed wetting failure as a function of both flow rate and substrate speed. In this instance there are apparently two wetting failure onset boundaries observable; a low speed boundary (b,c) and a high speed boundary (d–f). The low speed boundary is characterized by "V-shaped" air pockets formed at the wetting line (Blake and Ruschak, 1979). The size of the pockets scale with flow rate, however, they disappear at moderate flows (a). The high-speed boundary is characterized by catastrophic wetting failure associated with a highly roughened liquid surface. At

a moderate flow rate (3.2×10^{-4} m^2/s), as speed is progressively increased, wetting failure (small V-pockets —b) occurs at 0.45 m/s. As speed is increased further, these pockets disappear (0.75 m/s). Dynamic wetting with no evidence of air-entrainment then persists to a speed of 6.95 m/s when catastrophic failure occurs (e). As this high-speed failure starts, a large heel may also develop (Clarke, 1995). On slowing from this speed, the catastrophic wetting failure persists down to 3.40 m/s when dynamic wetting with no evidence of trapped air restarts (that is, there is hysteresis). Slowing further, the V-shaped pockets reappear at 0.75 m/s and subsequently disappear at 0.45 m/s. At a flow rate of 2.6×10^{-4} m^2/s, the V-pockets are not observed at all. At a much higher flow rate of 4.0×10^{-4} m^2/s, the V's are enlarged (c) and do not clear as speed is increased, they simply change character by joining and forming a chaotic pattern downstream (d).

A similar sequence is shown more explicitly in Figure 5. Here the liquid is aqueous glycerol of viscosity 100 mPas, the curtain height is 20 mm, and the flow rate is 5.0×10^{-4} m^2/s. The sequence shows in (a) small V-shaped air pockets at the wetting line. As speed is increased slightly in (b), the same, but fewer, air pockets are visible. In (c) the speed is such that there are no discernible air pockets and the process is apparently free of air-entrainment. As the speed is increased still further, catastrophic wetting failure occurs (d). Subsequently, as the substrate speed is reduced, (e), an air film downstream of the curtain impingement point is clearly seen as a uniform black area. As the speed is reduced further, (f) (g) and (h), areas of "touchdown" (that is, no air-entrainment) are seen which increase in number until dynamic wetting restarts completely.

It is well known by both coating practitioners (Blake and Ruschak, 1997) and scientists investigating wetting dynamics (Blake, 1993) that the maximum dynamic wetting speed obtainable in a given configuration is inversely related to viscosity of the liquid at the wetting line. However, the anomalous result of Figure 2 prompts us to confirm this dependence for a rough support. Figure 6 shows the variation with viscosity of the maximum speed obtained without air-entrainment at a flow rate of 4.2×10^{-4} m^2/s. Solutions of aqueous glycerol (Newtonian) containing a small amount (0.2%) of an inert blue dye were used. The support had a roughness of $R_z = 4.4$ μm. As viscosity is increased, initially the expected inverse dependence is seen. However, above a critical viscosity, no low speed wetting failure is seen and the wetting failure onset switches to high speed. This corresponds to the gap in the low speed boundary of Figure 4 widening as viscosity is increased. As viscosity is increased further, the maximum speed observed again falls.

It is also well known in the coating art that increasing curtain height can defer the onset of wetting failure. This effect is due to the momentum of the impinging sheet of liquid helping to drive wetting; hence, it is referred to as a hydrodynamic assist (Blake et al., 1994). Figure 7 shows the corresponding effect when coating on a rough support. Curtain heights of 10, 20, 30 and 40 mm have been used. In each case the coating liquid used was 194 mPas aqueous gelatin solution. This data can be normalized by dividing the onset speed

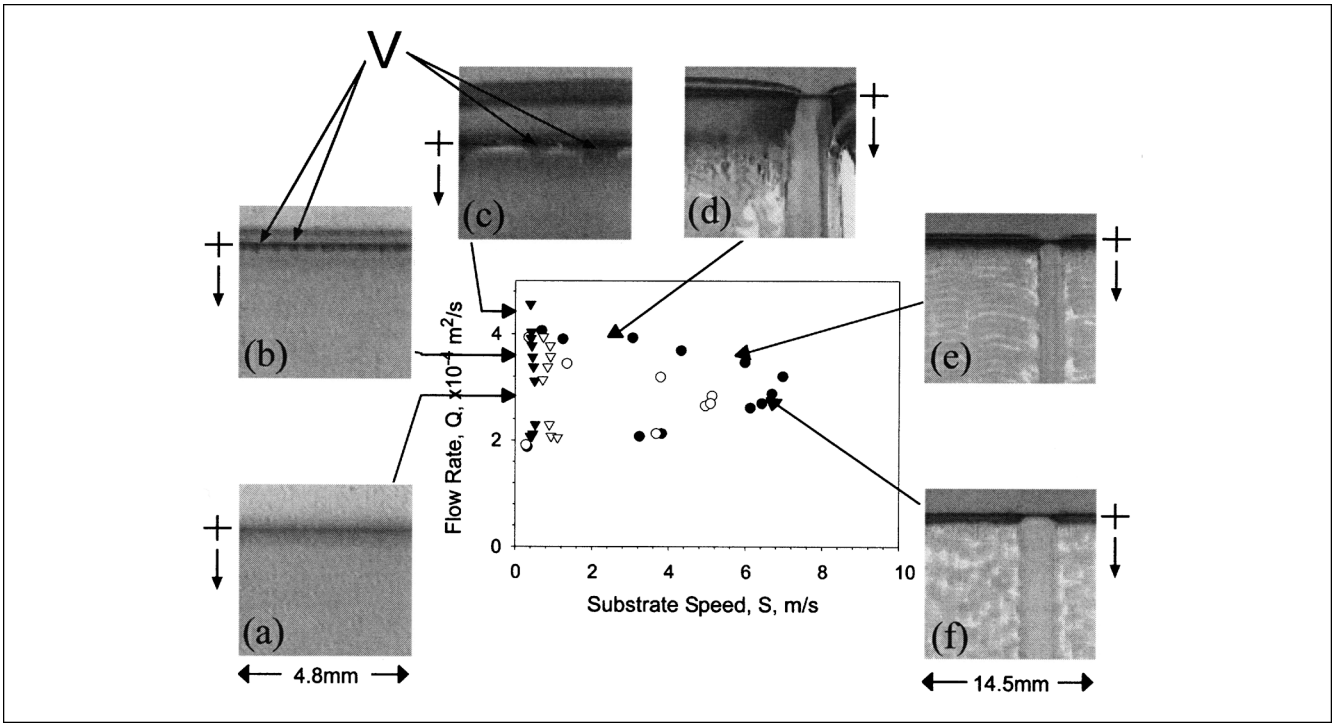

Figure 4. In-line images of coating obtained during a coating experiment (30 mm curtain height) on rough ($R_Z = 4.4$ μm) support.

The liquid used is aqueous glycerol of viscosity 57.4 m·Pa·s. In each image, the web moves from top to bottom as indicated and the approximate position of the wetting line is indicated by a +. (b,c) air entrainment with bubbles entrained from small "V" shaped wetting line pockets at low speed. (a) no low speed air entrainment observed. (d–f) gross failure at high speeds.

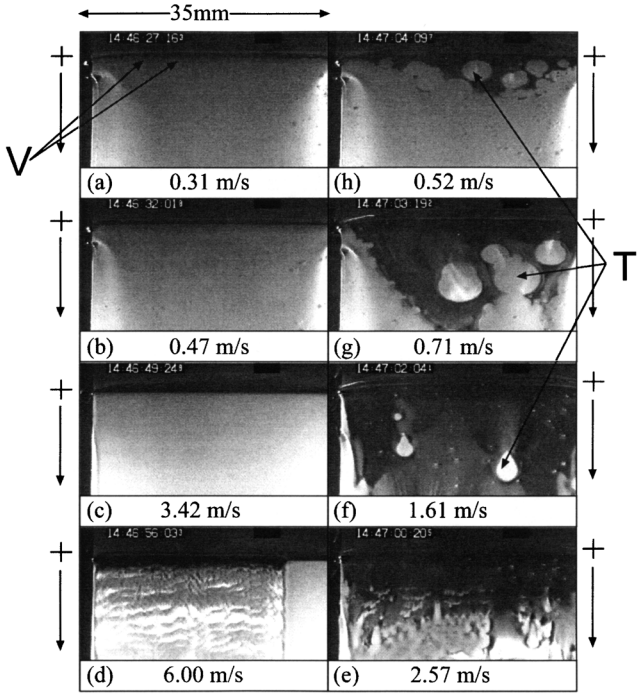

Figure 5. Sequence showing the progression of wetting failure as speed is varied during a coating experiment using 100 mPa·s aqueous glycerol, a 20 mm curtain height on a rough ($R_Z = 4.4\ \mu$m) surface.

In each case the substrate movement is indicated by an arrow, and the approximate location of the wetting line by a +. (a) air-entrainment "V"s at the wetting line; (b) number of air-entrainment "V"s reduce; (c) no observable air-entrainment; (d) catastrophic air-entrainment; (e) catastrophic air-entrainment persists as speed is reduced; (f) air-entrainment—apparent sheet of air with wetted areas (indicated with a T); (g) wetted areas increase in number as speed is reduced; (h) air sheet reduces in length until clear coating (not shown) with no evidence of air-entrainment restarts along the wetting line.

by the liquid impingement velocity raised to the power 1.2, Figure 8 (a simple model, from which this power is obtained, is described in the discussion below). The 10 mm data does not collapse well, probably because, at this height, the curtain is not yet in plug flow (Clarke et al., 1997). The value of 1.2 is almost double that observed previously (Blake et al., 1994) for hydrodynamic assist (0.66), moreover, the speeds here are much greater. This suggests that whereas hydrodynamic loading is a controlling factor leading to the high speeds, the mechanism is different to that observed previously.

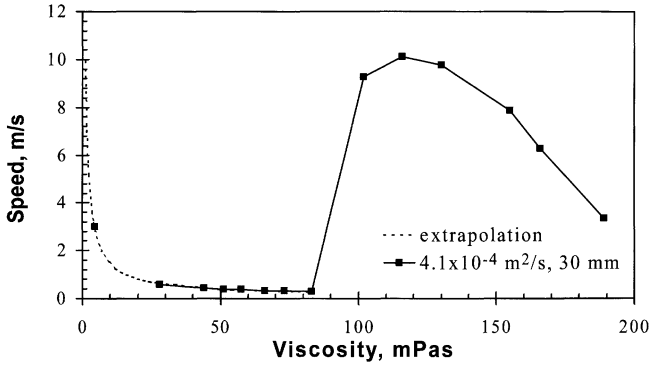

Figure 6. Anomalous behavior as a function of viscosity.

Maximum wetting speeds (highest speed boundary) observed for a curtain height 30 mm and flow rate of 4.2×10^{-4} m^2/s for various aqueous solutions of glycerol on a rough ($R_Z = 4.4\mu$m) surface.

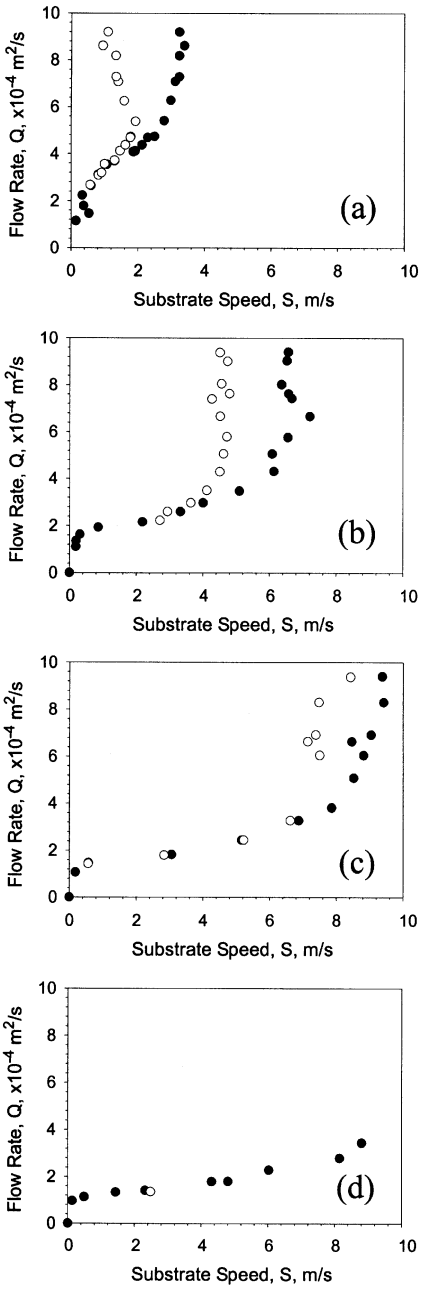

Figure 7. Coating maps for curtain heights (a) 10 mm, (b) 20 mm, (c) 30 mm and (d) 40 mm, coating on a rough ($R_Z = 4.4\mu$m) surface.

The liquid is aqueous gelatin with a low shear viscosity of 194 mPas. Solid symbols are for the onset of wetting failure on increasing web speed; open symbols are for the disappearance of wetting failure on reducing web speed.

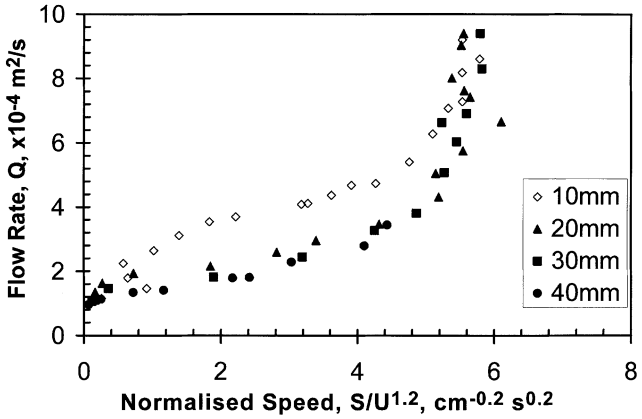

Figure 8. Air entrainment onset data from Figure 7 normalized by the liquid impingement speed, $U^{1.2}$.

Only the onset speeds are shown.

Having observed a new dynamic wetting regime and having demonstrated that substrate roughness is the key enabling factor, we investigate further the influence that the scale of roughness has on the observed wetting failure speed. For this purpose, we utilized a range of materials consisting of PE embossed with various random patterns. These patterns are characterized by R_Z values ranging from approximately 2 μm to 12 μm. Note that, chemically, these surfaces are nominally the same, so that the expected natural maximum wetting velocity should also be the same. The measured static advancing and receding contact angles are shown in Table 1. To compare the behavior of these surfaces, air-entrainment speeds were obtained for a single curtain height (20 mm) and a single flow rate (4.2×10^{-4} m^2/s) for a range of liquid viscosities (aqueous glycerol). The resulting data are plotted in Figure 9. The cross-section of this surface at a roughness of 4.4 μm corresponds to the data in Figure 8. It can be seen that an optimum exists as a function of both viscosity and roughness for which the coating speed reaches a maximum. Although this speed is plotted as the machine maximum of 1.15 m/s, it was in fact in excess of our experimental capabilities. If we take a section of this plot at constant viscosity, but above the threshold viscosity, then we find that there is a threshold roughness of approximately 2.5 μm. Above this value, the speed scales as approximately as $\sqrt{R_Z}$ up to about 10 μm when the speed again begins to fall. A section taken below the threshold viscosity shows the opposite behavior, that is, the air-entrainment speed falls as R_Z increases.

Discussion

On a rough surface, we observe a switch to a second dynamic wetting mechanism. This switch is characterized by a sudden increase in the maximum wetting speed as a function of liquid viscosity. The second mechanism is, however, only seen when liquid viscosity, surface roughness, and curtain height are all within the appropriate ranges. The dependence of wetting failure speed on these key parameters can be qualitatively described by a mechanism whereby a small amount of air is trapped within the topography of the substrate. This air leads to a composite interface that might be likened to a very low viscosity layer sandwiched between the coating liquid and the substrate. The amount of air that is trapped being controlled both by the topography of the substrate and the pressure squeezing the liquid against the substrate. Thus, a dependence of maximum coating speed on both substrate roughness and curtain height may be derived.

Table 1. Measured Static Advancing and Receding Contact Angles

R_z	0.6 μm (PET)	1.9 μm	2.5 μm	2.8 μm	4.4 μm	9.6 μm	12.7 μm
Receding Angle	50	71	69	83	74	72	71
Advancing Angle	72	82	85	91	91	100	79

Blake and Ruschak (1997) and, earlier, Teletzke et al. (1988) have calculated the thickness of an air film entrained between a loaded liquid and a smooth substrate. Their model accords with intuition in that such an air film thickens with increasing substrate speed and thins with increasing load. The final air film thickness H_A^∞ is given by Blake and Ruschak as

$$H_A^\infty = \frac{\gamma}{P_L}\left[\frac{3\sqrt{2}\,(1+m)}{8}\left(\frac{\eta_A}{\gamma}\right)\right]^{2/3} \tag{1}$$

where γ is the liquid surface tension, P_L is the load pressure, η_A is the viscosity of air, S is the substrate speed, and m is the ratio of the liquid to substrate speed. For an air film which has a similar scale to the roughness, the coating will be made on a composite surface composed of air and solid (Menchaca-Rocha, 1992; Miwa et al., 2000). In this case the stress σ at the interface accelerating the liquid may be written

$$\sigma = \eta\frac{dv_x}{dy} = \eta_E\frac{S-V}{H} \tag{2}$$

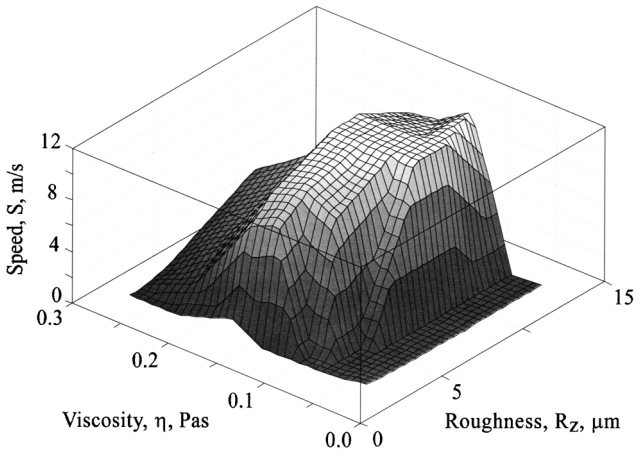

Figure 9. Maximum wetting failure speed at a flow rate of 4.2×10^{-4} m^2/s and curtain height of 20 mm as a function of roughness and viscosity.

The liquids are various concentrations of aqueous glycerol and the surfaces are embossed polyethylene.

where η_E is an effective viscosity due to the composite nature of the interface (areas of air-liquid and areas of solid-liquid), H is the average composite film thickness ($< R_Z$), and V is the effective interface velocity. This stress is responsible for accelerating the liquid to the substrate speed, therefore, assuming the stress is continuous at the composite interface

$$\eta_E \frac{S-V}{H} = \eta \frac{V}{D} \tag{3}$$

where η is the liquid viscosity and D is the entrained liquid depth. The liquid flow rate is $Q = SD$. The effective interface velocity V will be close to zero at the contact line and will be equal to S when the liquid is fully entrained; thus, over the distance the interface is accelerated, the average velocity is $S/2$, hence

$$SH = \frac{\eta_E}{\eta} Q \tag{4}$$

For a given surface, the maximum air film thickness will be R_Z and, for greater air-film thicknesses, the liquid must disconnect from the substrate and wetting failure will ensue. Thus, there is a speed S_Z corresponding to this average air-film thickness. Taking η_E as independent of wetting failure speed, the righthand side of Eq. 4 is independent of substrate speed and we can, therefore, equate the lefthand side of Eq. 4 for two conditions S_Z and S. Equating H with H_A^∞, this then gives the maximum air film thickness before wetting failure at speed S as

$$H_A^\infty \approx \frac{R_Z S_Z}{S} \tag{5}$$

Combining this with Eq. 1 leads to a prediction of the maximum speed obtainable before failure of the wetting process $S_{\max}$ as

$$S_{\max} = \left[\left(\frac{8\gamma}{3\sqrt{2}\,(1+m)\eta_A} \right)^{2/3} \frac{R_Z S_Z P_L}{2\gamma} \right]^{3/5} \tag{6}$$

This equation predicts extremely high wetting speeds, albeit the process necessitates a quantity of air to be trapped within the topography of the substrate. In a curtain coating process the load pressure might be of order 5,000 Pa, the roughness, 5×10^{-6} m, the normal maximum wetting speed 5 m/s, and the surface tension 0.05 N/m. The viscosity of air is approximately 2×10^{-5} Pas, so taking m as 1 for worst case and equating the normal maximum wetting speed with S_Z, $S_{\max} \approx$ 40 m/s. It might be noted that this speed is comparable to that used in typical paper coating processes (Becker et al., 2000), but is much greater than that expected for even a favorable wetting situation (water coating on PET, $S_{\max} \approx 10$ m/s (Blake, 1993)).

From Eq. 6, we can deduce the expected behavior of wetting failure speed on the main parameters of roughness and load pressure. For roughness, the maximum coating speed is expected to behave as $S_{\max} \alpha R_z^{0.6}$. Over a certain range of roughness, this qualitative behavior is seen. For load pressure, we take P_L to be $P_L \approx 0.25\ \rho U^2$ and $U = \sqrt{(U_0^2 + 2\ gh)}$ is the liquid impingement velocity with h the curtain height to give

$$S_{max} \propto U^{1.2} \propto \left(U_0^2 + 2gh \right)^{0.6} \tag{7}$$

Hence, the dependence on curtain height observed in Figures 7 and 8. Note that, although Eqs. 6 and 7 contain no explicit flow rate dependence, it should be expected that the flow rate will alter the pressure at the base of the curtain P_L in a complex fashion.

Conclusions

The data presented here unequivocally demonstrate that a mechanism different to that usually referred to as dynamic wetting can be induced on a rough substrate. That is, the two observed boundaries in Figure 4, and the large step in speed as a function of viscosity in Figure 6, are not explained by our conventional understanding of dynamic wetting. In addition to roughness, the observed requirements to induce this second mechanism include a load pressure close to the nominal wetting line and a high liquid viscosity. Similar effects have been observed previously with nonwetting droplets sliding on the crests of a surface topography (Herminghaus, 2000; Menchaca-Rocha, 1992; Miwa et al., 2000). In the present case, however, rather than being hydrophobic ($\theta > 90°$), the substrates are slightly hydrophilic ($\theta < 90°$), although it might be noted that the dynamic contact angles in a high-speed coating process are likely to be significantly greater than 90°.

The coating literature describes a concept whereby coating is always associated with an entrained air film (Miyamoto, 1991). While this is attractive from a continuum hydrodynamical point of view, since it automatically relaxes the no-slip boundary condition at the three-phase line and so avoids a singularity problem (Blake and Ruschak, 1997; Huh and Scriven, 1971; Dussan and Davis, 1974), it fails to predict the discontinuous step in behavior obvious in the data presented here. Indeed, no simple wetting mechanism predicts such a discontinuous step. Hence, it seems probable that the two distinct mechanisms described here each exist in different parameter regimes.

Acknowledgments

The author would like to thank K. Goppert for supply of many of the substrate materials, K. J. Ruschak for prompting this line of research, and both T. D. Blake and C. L. Bower for many useful discussions.

Literature Cited

Becker, I., H. Sommer, and K. Stränger, "Trends in Coating Technology for Paper and Board Grades Requiring First-Class Surface Coverage," TAPPI Coating Conference, Washington, DC, published by TAPPI Press, Atlanta, GA (May 1–4, 2000).

Blake, T. D., "Dynamic Contact Angles and Wetting Kinetics," *Wettability*, J. C. Berg, ed., Marcel Dekker, New York (1993).

Blake, T. D., A. Clarke, and K. J. Ruschak, "Hydrodynamic Assist of Dynamic Wetting," *AIChE J.*, **40**, 229 (1994).

Blake, T. D., R. Dobson, G. N. Batts, and W. J. Harrison, "Coating Processes," U.S. Patent No. 5,391,401 (1993).

Blake, T. D., and K. J. Ruschak, "A Maximum Speed of Wetting," *Nature*, **282**, 489 (1979).
Blake, T. D., and K. J. Ruschak, "Wetting: Static and Dynamic Contact Lines," *Liquid Film Coating*, S. F. Kistler and P. M. Schweizer, eds., Chapmans Hall, London (1997).
Buonopane, R. A., E. B. Gutoff, and M. M. T. Rimore, "Effect of Plunging Tape Surface Properties on Air-Entrainment Velocity," *AIChE J.*, **32**(4), 682 (1986).
Burley, R., and R. P. S. Jolly, "Entrainment of Air into Liquids by a High-Speed Continuous Solid Surface," *Chem. Eng. Sci.*, **39**, 1357 (1984).
Clarke, A., "Recirculating Flows in Curtain Coating," P. H. Gaskell, *The Mechanics of Thin Film Coatings*, M. D. Savage, and J. L. Summers, eds., World Scientific, Singapore (1995).
Clarke, A., T. D. Blake, and K. J. Ruschak, U.S. Patent No. 6,099,913 (1998).
Clarke, A., S. J. Weinstein, A. Moon, and E. A. Simister, "Time-Dependent Equations Governing the Shape of a Two-Dimensional Liquid Curtain, Part 2: Experiment," *Phys. Fluids*, **9**, 3637 (1997).
Cox, R. G., "The Dynamics of the Spreading of Liquids on a Solid Surface," *J. Fluid Mech.*, **168**, 169 (1986).
Dettre, R. H., and R. E. Johnson, "Contact Angle Measurements on Rough Surfaces," *Contact Angle Wettability and Adhesion*, F. M. Fowkes, ed., Advances in Chemistry Series, No. 43, ACS, Washington, DC (1964).
Deutsche Norm DIN 4768 (1990); International standard ISO 4287 (1997).
Dussan, E. B. V, and S. H. Davis, "On the Motion of a Fluid-Fluid Interface Along a Solid Surface," *J. Fluid Mech.*, **65**, 71 (1974).
Gutoff, E. B., and C. E. Kendrick, "Dynamic Coating Angles," *AIChE J.*, **28**, 456 (1982).
Herminghaus, S., "Roughness-Induced Non-Wetting," *Europhys. Lett.*, **52**, 165 (2000).
Huh, C., and L. E. Scriven, "Hydrodynamic Model of Steady Movement of a Solid/Liquid/Fluid Contact Line," *J. Coll. Intf. Sci.*, **35**, 85 (1971).
Johnson, R. E., and R. H. Dettre, "Study of an Idealized Rough Surface," *Contact Angle Wettability and Adhesion*, F. M. Fowkes, ed., Adv. in Chemistry Ser., No. 43. ACS (1964).
Menchaca-Rocha, A., "The Mobility of Mercury Drops on Rough Glass Surfaces," *J. Coll. Intf. Sci.*, **149**, 472 (1992).
Miwa, M., A. Nakajima, A. Fujishima, K. Hashimoto, and T. Watanabe, "Effects of the Surface Roughness on Sliding Angles of Water Droplets on Superhydrophobic Surfaces," *Langmuir*, **16**, 5754 (2000).
Miyamoto, K., "On the Mechanism of Air-Entrainment," *Ind. Coating Res.*, **1**, 71 (1991).
Palasantzas, G., "Wetting on Rough Self-Affine Surfaces," *Phys. Rev. B*, **51**(20), 14612 (1995).
Rolley, E., C. Guthmann, R. Gombrowicz, and V. Repain, "Roughness of the Contact Line on a Disordered Substrate," *Phys. Rev. Lett.*, **80**(13), 2865 (1998).
Shikhmurzaev, Y. D., "Moving Contact Lines in Liquid/Liquid/Solid Systems," *J. Fluid Mech.*, **334**, 211 (1997).
Suga,Y., K. Nakajima, K. Kobayashi, and K. Miyamoto, U.S. Patent No. 5,393,571 (1993).
Teletzke, G. F., H. T. Davis, and L. E. Scriven, "Wetting Hydrodynamics," *Revue Phys. Appl.*, **23**, 989 (1988).
Voinov, O. V., "Hydrodynamics of Wetting," *Fluid Dyn.*, **11**, 714 (1976).
Zhou, X. B., and J. Th. M., "Influence of Surface Roughness on the Wetting Angle," *J. Mater. Res.*, **10** 1984 (1995).

Manuscript received Oct. 2, 2001, and revision received Mar. 15, 2002.